Published OnlineFirst April 6, 2010; DOI: 10.1158/1535-7163.MCT-10-0055
Published Online First on April 6, 2010 as 10.1158/1535-7163.MCT-10-0055

Research Article

Molecular Cancer Therapeutics

Preclinical Antitumor Activity of the Orally Available Heat Shock Protein 90 Inhibitor NVP-BEP800

Andrew J. Massey[1], Joseph Schoepfer[2], Paul A. Brough[1], Josef Brueggen[2], Patrick Chène[2], Martin J. Drysdale[1], Ulrike Pfaar[3], Thomas Radimerski[2], Stephan Ruetz[2], Alain Schweitzer[2], Mike Wood[1], Carlos Garcia-Echeverria[2], and Michael Rugaard Jensen[2]

Abstract

Heat shock protein 90 (Hsp90) is a ubiquitously expressed molecular chaperone with ATPase activity involved in the conformational maturation and stability of key signaling molecules involved in cell proliferation, survival, and transformation. Through its ability to modulate multiple pathways involved in oncogenesis, Hsp90 has generated considerable interest as a therapeutic target. NVP-BEP800 is a novel, fully synthetic, orally bioavailable inhibitor that binds to the NH_2-terminal ATP-binding pocket of Hsp90. NVP-BEP800 showed activity against a panel of human tumor cell lines and primary human xenografts *in vitro* at nanomolar concentrations. In A375 melanoma and BT-474 breast cancer cell lines, NVP-BEP800 induced client protein degradation (including ErbB2, B-Raf^{V600E}, Raf-1, and Akt) and Hsp70 induction. Oral administration of NVP-BEP800 was well tolerated and induced robust antitumor responses in tumor xenograft models, including regression in the BT-474 breast cancer model. In these tumor models, NVP-BEP800 modulated Hsp90 client proteins and downstream signaling pathways at doses causing antitumor activity. NVP-BEP800 showed *in vivo* activity in a variety of dosing regimens covering daily to weekly schedules, potentially providing a high degree of flexibility in dose and schedule within the clinical setting. Overall, given the mechanism of action, preclinical activity profile, tolerability, and pharmaceutical properties, NVP-BEP800 is an exciting new oral Hsp90 inhibitor warranting further development. *Mol Cancer Ther; 9(4); 906–19. ©2010 AACR.*

Introduction

Considering the molecular complexity of cancer with multiple genetic abnormalities and the ability to develop resistance to current therapies, targeting pathways by inhibiting the activity of a single component is unlikely to be effective long term. The identification of molecular targets that modulate multiple components of one or several signaling pathways in a nongenotoxic manner is highly desirable for anticancer drug discovery. Heat shock protein 90 (Hsp90) has attracted considerable interest in recent years as such a potential therapeutic target for the identification and development of a new generation of anticancer drugs (1–5). The Hsp90 family of molecular chaperones is a ubiquitously and widely expressed family of protein chaperones comprising cytosolic Hsp90α and Hsp90β, endoplasmic reticulum Grp94, and mitochondrial Trap-1 (6, 7). In the cell, Hsp90α and Hsp90β exist as large multiprotein complexes in cohort with a variety of co-chaperones, including Aha1, Hsp70, Hop, Hip, Cdc37, and p23. The ATPase activity of Hsp90, in addition to its various co-chaperones, is essential for maintaining the conformational maturation, stability, and activity of a variety of "client" proteins, including many key proteins necessary for the oncogenic phenotype. The mechanism by which Hsp90 functions is complex, requiring the sequential binding and dissociation of various co-chaperones as well as the hydrolysis of ATP to drive the chaperone cycle (7, 8).

Hsp90 is an exciting target for anticancer therapeutics, as inhibiting it has the potential to affect all the hallmarks of cancer (9). The natural products geldanamycin and radicicol both bind to and inhibit the NH_2-terminal ATPase of Hsp90, resulting in the proteasomal degradation of client proteins (10). Degradation of these oncogenic client proteins results in both tumor cell growth arrest and death (11). The semisynthetic geldanamycin analogue 17-allylamino-17-demethoxygeldanamycin (17-AAG) has provided further validation for Hsp90 as a target through preclinical and clinical studies. This first-in-class Hsp90 inhibitor, along with the hydroquinone prodrug IPI-504, has shown evidence of target modulation in

Authors' Affiliations: [1]Vernalis Ltd., Cambridge, United Kingdom and [2]Novartis Institutes for BioMedical Research; and [3]Novartis Pharma AG, Basel, Switzerland

Note: Supplementary materials for this article are available at Molecular Cancer Therapeutics Online (http://mct.aacrjournals.org/).

Current address for M.J. Drysdale: The Beatson Institute for Cancer Research, Glasgow, United Kingdom.

Corresponding Author: Michael Rugaard Jensen, Novartis Institutes for BioMedical Research, Novartis Pharma AG, Klybeckstrasse 141, WKL-125.2.42, CH-4057 Basel, Switzerland. Phone: 41-61-696-78-65; Fax: 41-61-696-57-51. E-mail: michael_rugaard.jensen@novartis.com

doi: 10.1158/1535-7163.MCT-10-0055

Published OnlineFirst April 6, 2010; DOI: 10.1158/1535-7163.MCT-10-0055

melanoma, prostate, renal, multiple myeloma, and trastuzumab-refractory breast cancer (5, 12). Despite the clinical progression of 17-AAG, this compound, and those based on the ansamycin scaffold, has potential limitations, including poor solubility, necessitating complex formulations or the prodrug approach, limited bioavailability, and hepatotoxicity (13–15). Some of the formulations required to administer 17-AAG may contribute to its dose-limiting toxicity (16). In addition, it is also of concern that resistance to 17-AAG can be acquired through P-glycoprotein upregulation or by mutation or loss of the *NQO1* gene [NAD(P)H:quinone oxidoreductase 1, DT-diaphorase], which is required for the bioreduction of 17-AAG into its more potent hydroquinone metabolite (17–20). To overcome the limitations of the ansamycin-derived Hsp90 inhibitors, the identification of a non-ansamycin, fully synthetic small-molecule inhibitor binding in the ATP pocket of Hsp90 would be of great therapeutic interest. New agents suitable for i.v. administration, including NVP-AUY922 (Novartis/Vernalis), AT13387 (Astex), and STA-9090 (Synta), or the oral route, including BIIB021 (Biogen Idec), PF-04929113 (SNX5422, Pfizer), XL888 (Exelixis), or IPI-493 (Infinity), are in clinical development. Additional agents are undergoing preclinical development and predicted to enter the clinic in the near future (5). We have previously described the discovery of a novel series of orally bioavailable 2-aminothieno [2,3-*d*]pyrimidine–based Hsp90 inhibitors using fragment-based and *in silico* screening (21). We now report on the *in vitro* activity and *in vivo* pharmacokinetic, pharmacodynamic, and efficacy profiles of NVP-BEP800 in human cancer cell lines of different etiology. These results support the selection of NVP-BEP800 for clinical development.

Materials and Methods

Compounds

NVP-BEP800 and NVP-AUY922 were synthesized as previously described (21, 22). For *in vitro* studies, 10 mmol/L stock solutions were prepared in 100% DMSO and stored at −20°C. For *in vivo* studies, NVP-BEP800 was formulated as a suspension in 0.5% methyl cellulose and NVP-AUY922 was formulated as a solution consisting of 5% glucose in water. Compounds were administered to mice in a dose volume of 10 mL/kg.

Hsp90 binding and selectivity assays

Activity was determined against Hsp90β, Hsp70, Grp94, and Trap-1 using a competitive fluorescent polarization assay as previously described (23). Activity against topoisomerase II was done as previously described (24). The activity of NVP-BEP800 was evaluated against a panel of kinases consisting of HER-1, KDR, Flt-3, IGF-1R, Tek, c-src, c-Met, Ret, JAK-2, EphB4, FGFR-3-K650E, Axl, FAK, c-Abl, c-Abl-T315I, PKA, CDK1/B, PKB/Akt, PDK1, and B-Raf-V599E.

Cell proliferation and clonogenic assays

Unless otherwise stated, all cell lines were obtained from the American Type Culture Collection and grown in recommended medium in a humidified atmosphere of 5% CO_2 in air. Cell proliferation was determined using either sulforhodamine B for adherent cells or MTS assay for suspension cells or those showing low adherence. GI_{50} was the compound concentration that inhibits cell growth by 50% compared with vehicle control. Cell death was determined using a ToxiLight nondestructive cytotoxicity bioassay kit (Lonza). LD_{50} was the compound concentration that induced 50% of the maximal death. Caspase-3/7 activity was determined using a homogeneous caspase activity kit (Promega). Cell cycle progression was determined by RNase A/propidium iodide staining following fixation in 70% ethanol. Data were collected on a FACSArray cytometer and analyzed with FACSDiva software (BD Biosciences). A clonogenic assay from serially passaged human tumors was done in a 24-well format as described (Oncotest GmbH; ref. 25). Briefly, serially passaged solid human xenografts growing subcutaneously in nude mice (NMRI *nu/nu* strain) were disaggregated, and 4×10^4 to 8×10^4 viable cells were added to 0.2 mL of Iscove's medium [supplemented with 20% (v/v) FCS and 1% (v/v) gentamicin] containing 0.4% agar and plated on top of the base layer (0.75% agar). After 24 h, the drug was added in an additional 0.2 mL of medium and incubated at 37°C in a humidified atmosphere containing 7.5% CO_2. At the time of maximum colony formation (8–20 d), counts were done with an automatic image analysis system (OMNICON FAS IV; Bio-Sys GmbH).

Western blot analysis and immunoprecipitation

Client protein degradation was determined by Western blot analysis as previously described (26). ErbB2 (Abcam), Raf-1 (Santa Cruz Biotechnology), phospho-Akt (Ser^{473}; Cell Signaling Technology, Inc.), Akt (Cell Signaling Technology), phospho-mitogen-activated protein/extracellular signal-regulated kinase kinase (MEK) 1/2 (Cell Signaling Technology), and Hsp70 (StressGen) levels were determined using enhanced chemiluminescence (GE Bioscience). Glyceraldehyde-3-phosphate dehydrogenase (Chemicon International) levels were determined to evaluate equal protein loading. p23 immunoprecipitation was carried out essentially as described previously (26).

Pharmacokinetic analysis

Female athymic BT-474 tumor-bearing mice with tumors of ~250 mm^3 received a single dose of NVP-BEP800. At various time points, mice ($n = 4$) were sacrificed and blood and tissues (tumor, liver, lung, heart, and muscles) were dissected. Concentrations of NVP-BEP800 in plasma and tissue were determined by high-pressure liquid chromatography/tandem mass spectrometry (HPLC/MS-MS), following the basic procedure described (26). Briefly, following chromatographic separation, the

Published OnlineFirst April 6, 2010; DOI: 10.1158/1535-7163.MCT-10-0055

column eluent was directly introduced into the ion source of the triple quadrupole mass spectrometer Quattro Ultima (Micromass) controlled by Masslynx 4.0 software. Electrospray positive ionization (ESI+) multiple reaction monitoring was used for the MS/MS detection of the analyte NVP-BEP800. Precursor-to-product ion transitions of m/z 480.35→m/z 435.15 for NVP-BEP800 and m/z 492.35→m/z 435.20 for an internal standard were used. The limit of quantification was set to 10 ng/mL and 10 ng/g for plasma and tissues, respectively (coefficient of variation and overall bias of <30%). Regression analysis and further calculations were done using QuanLynx 4.0 (Micromass) and Excel 2002 (Microsoft). Concentrations of unknown samples were back calculated based on the peak area ratios of analyte/internal standard from a calibration curve constructed using calibration samples spiked in blank plasma or tumor tissue obtained from untreated (not dosed) animals. Assay linearity was indicated by an overall regression coefficient of 0.9363. Pharmacokinetic parameters were calculated from the mean individual values by using a noncompartmental model for i.v. or extravascular dosing (WinNonlin Professional version 4.0, Pharsight Corp.). Areas under the plasma/tissue concentration versus time curves (AUC) were calculated with linear trapezoidal rule.

Quantitative whole-body autoradioluminography

The tissue distribution of radioactivity was assessed by quantitative whole-body autoradioluminography (27) at 0.083, 0.5, 2, 4, 8, 24, 48, 72, 96, and 168 h after dosing (n = 1 mouse per time point). Several 40-μm sagittal sections were obtained in a CM 3600 cryomicrotome (Leica Biosystems GmbH) according to the method of Ullberg (28). A block of ^{14}C-radiolabeled standards, prepared in blood and assayed by liquid scintillation counting, was sectioned in the same manner and on the same day as the mice were sectioned. Following dehydration, tissue and standard sections were exposed to Fuji BASIII Imaging plates (GE Healthcare, formerly Fuji Photo Film Co. Ltd.) or to SR screens (Perkin-Elmer, formerly Packard Instrument) for 1 d at room temperature in a lead shielded box to minimize the background signal. The levels of radioactivity were determined by comparative densitometry and digital analysis of the autoradiograms according to Schweitzer et al. (29) using a MCID/Elite (6.0) image analyzer (Imaging Research). The limit of detection (LOD; 0.26 nmol/g) was set equal to the mean of background + 3 SD, and the quantification limit (0.78 nmol/g) was taken as 3 × LOD.

Human xenograft models and antitumor efficacy studies

The estrogen receptor (ER)–positive, ErbB2-overexpressing cell line BT-474 was purchased from the American Type Culture Collection. The cells were grown in DMEM high glucose (4.5 g/L) supplemented with 10% FCS, 200 mmol/L L-glutamine, and 1% sodium pyruvate (BioConcept). Two or 3 d before cell inoculation, each mouse was s.c. implanted on the upper dorsal side with a 17β-estradiol pellet (25 μg/d; 90-d release; Innovative Research of America) using a trocar needle. BT-474 cells (5×10^6) were injected in 200 μL Matrigel/HBSS (1:1 volume; BD Matrigel Basement Membrane Matrix, BD Biosciences) s.c. in the right flank. The A375 cell line expresses mutant B-Raf (V600E; refs. 30, 31). The cells were grown in RPMI 1640 supplemented with 10% FCS and 200 mmol/L L-glutamine. Cell culture reagents were purchased from BioConcept. To establish tumors, 5×10^6 A375 cells were injected s.c. in 200 μL PBS in the right flank. Invasive procedures were done under Forene anesthesia. All experiments were done using female Harlan HsdNpa: Athymic Nude-nu mice, which were obtained from Novartis internal breeding stocks (Laboratory Animal Services, Novartis Pharma AG, Basel, Switzerland). The animals were kept under optimized hygienic conditions with a 12-h dark, 12-h light cycle. The animals were fed food and water *ad libitum*. All animal experiments were done in adherence to the Swiss law for animal protection. The experimental protocols were approved by the Swiss Kantonal Veterinary Office of Basel Stadt (Basel, Switzerland).

Tumor volume measurements

Tumor growth and body weights were monitored at regular intervals. The xenograft tumor sizes were measured manually with calipers, and the tumor volume was estimated using the following formula: ($W \times L \times H \times \pi/6$), where width ($W$), length ($L$), and height ($H$) are the three largest diameters (32). Treatment with NVP-BEP800 was initiated when the average tumor volume reached 100 to 300 mm^3.

Statistical analysis

When applicable, results are presented as mean ± SEM. Tumor and body weight data were analyzed by ANOVA with post hoc Dunnett's test for comparison of treatment versus control group. The post hoc Tukey test was used for intragroup comparison. Statistical analysis was done using GraphPad Prism 5 (GraphPad Software). As a measure of efficacy, the %T/C value is calculated at the end of the experiment according to the following formula: (Δtumor volume$_{treated}$/Δtumor volume$_{control}$) × 100, where Δtumor volumes represent the mean tumor volume on the evaluation day minus the mean tumor volume at the start of the experiment. If tumor regression was observed, % regression was calculated relative to the initial mean tumor volume.

Results

NVP-BEP800 is a potent and selective Hsp90 inhibitor

NVP-BEP800 was discovered through a rational design approach, where fragment-based lead finding was combined with *in silico* screening and X-ray crystallography (21). NVP-BEP800 is of a chemical class distinct from

Published OnlineFirst April 6, 2010; DOI: 10.1158/1535-7163.MCT-10-0055

Table 1. Structure and *in vitro* activity of NVP-BEP800 and NVP-AUY922

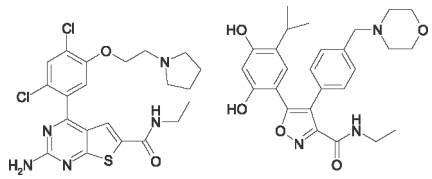

NVP-BEP800 NVP-AUY922

	Hsp90β, IC_{50} (μmol/L)	Grp94, IC_{50} (μmol/L)	Trap-1, IC_{50} (μmol/L)
NVP-BEP800	0.058 ± 0.006	4.1 ± 1.1	5.5 ± 0.48
NVP-AUY922	0.021 ± 0.006	0.54 ± 0.029	0.85 ± 0.004

NOTE: Chemical structures of NVP-AUY922 (left) and NVP-BEP800 (right). Competitive binding fluorescence polarization assays were used to determine the concentrations of NVP-AUY922 and NVP-BEP800, which inhibit Hsp90β, Grp94, and Trap-1 by 50% (IC_{50}). Values are the average of at least three independent determinations ± SEM.

NVP-AUY922, which has been described previously (22, 26). The chemical structures of these two Hsp90 inhibitors are shown in Table 1. In a competitive binding fluorescence polarization assay (23), NVP-BEP800 inhibited Hsp90β with an IC_{50} of 0.058 ± 0.006 μmol/L, 2.8-fold less potent than NVP-AUY922 (IC_{50}, 0.021 ± 0.006 μmol/L; ref. 22). NVP-AUY922 was moderately selective versus the Hsp90 family members Grp94 and Trap-1, with IC_{50}s of 0.54 ± 0.029 and 0.85 ± 0.004 μmol/L, respectively. In comparison, NVP-BEP800 was >70-fold selective against Grp94 and Trap-1, with IC_{50}s of 4.1 ± 1.1 and 5.5 ± 0.48 μmol/L. The selectivity of NVP-BEP800 was further ascertained against a diverse panel of protein kinases and showed an IC_{50} of >10 μmol/L against all 20 kinases. Additionally, a closely related GHKL ATPase, topoisomerase II, and a structurally unrelated ATPase, Hsp70, were screened at 10 μmol/L. Neither ATPase was inhibited by NVP-BEP800 at this concentration.

NVP-BEP800 inhibits proliferation of tumor cell lines and primary tumors *in vitro*

NVP-BEP800 was a potent inhibitor of tumor cell proliferation with GI_{50}s ranging from 38 nmol/L in A375 to 1,050 nmol/L in PC3, with an average GI_{50} of 245 nmol/L (Supplementary Table S1). As observed in the fluorescence polarization assay, the potency of NVP-BEP800 was lower than NVP-AUY922 (GI_{50} range, 2.3–49.6 nmol/L). In the panel tested, breast- and melanoma-derived cell lines were relatively sensitive to Hsp90 inhibition, warranting the further investigation of NVP-BEP800 in these tumor types.

The anticancer activity of NVP-BEP800 was also evaluated in 46 primary human tumors serially passaged in nude mice and three preparations of hematopoietic stem cells *in vitro* using a clonogenic assay. The 11 human tumor types included in the panel were bladder, colon, liver, non–small cell lung (adeno, squamous epithelium, and large cell), small cell lung, mammary, ovary, pancreatic, and renal cancer as well as melanoma and pleura mesothelioma. The mean IC_{50} and IC_{70} for NVP-BEP800 were determined to be 0.75 and 1.8 μmol/L, respectively (Supplementary Table S2). Within this primary tumor panel, small cell lung, mammary cancer, and melanoma showed above-average sensitivity to NVP-BEP800, whereas renal cell carcinoma showed below-average sensitivity.

NVP-BEP800 induces cell death and apoptosis in human breast cancer cell lines

Treatment of A2058 or A549 cells with five times the GI_{50} of NVP-BEP800 resulted in accumulation of cells in the G_2-M phase of the cell cycle (Fig. 1A). In A2058 cells, the percentage of cells in G_2-M increased from 22.2% to 51.7% and in A549 cells from 11.4% to 45.0% following NVP-BEP800 treatment. No obvious cell cycle arrest was observed in either HCT116 or BT-474 cells. However, treatment with NVP-BEP800 for 24 hours increased the percentage of cells, with sub-G_1 DNA content indicative of apoptosis induction. This was particularly marked in the BT-474 cell line, where NVP-BEP800 exposure increased the sub-G_1 fraction from 0.3% to 43.0%. In the other three cell lines tested, this increase was less dramatic, with the sub-G_1 population increasing by 12.1% in HCT116, 5.9% in A2058, and 7.1% in A549 cells.

Although breast cancer cell lines were among the most sensitive to NVP-BEP800 inhibition, the sensitivity of NVP-BEP800 was significantly reduced compared with NVP-AUY922, with an average GI_{50} of 120 nmol/L versus 5.4 nmol/L (26). Human cancer cell lines undergo various cell fates in response to Hsp90 inhibition (i.e., cytostasis, apoptosis, or cell death). In response to Hsp90 inhibition by NVP-BEP800 or NVP-AUY922, BT-474, MDA-MB-231, MDA-MB-468, and BT20 cells underwent

Published OnlineFirst April 6, 2010; DOI: 10.1158/1535-7163.MCT-10-0055

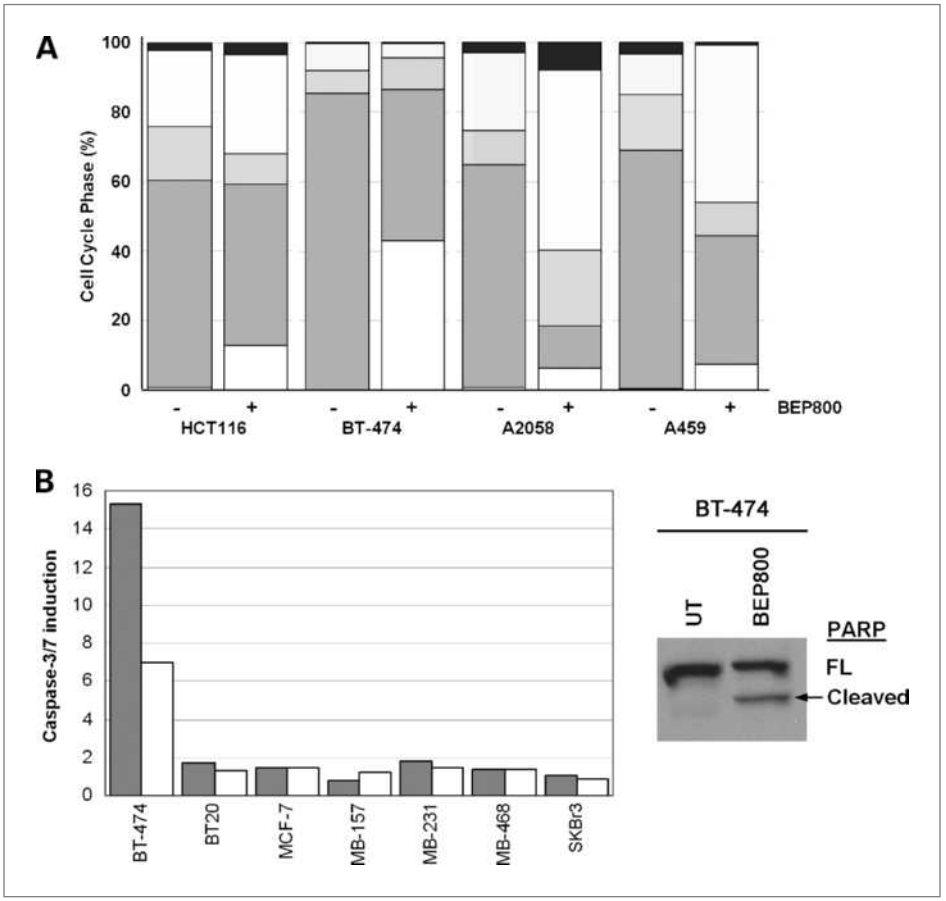

Figure 1. NVP-BEP800 induces cell cycle arrest, apoptosis, and cell death in a panel of human breast cancer cell lines. A, cell cycle analysis following DMSO (–) or five times the GI_{50} of NVP-BEP800 (+) exposure for 24 h. The percentage of cells in sub-G_1 (white), G_1 (gray), S (hatched), G_2-M (dotted), and >G_2-M (black) phases of the cell cycle are indicated. B, human breast cancer cells were exposed to five times the GI_{50} of NVP-BEP800 (gray columns) or NVP-AUY922 (white columns) for 24 h. The levels of active caspase-3/7 were determined using a homogeneous caspase kit. Levels of cleaved poly(ADP-ribose) polymerase (PARP) were determined by Western blotting in BT-474 cells following 24-h exposure to five times the GI_{50} of NVP-BEP800.

cell death, with LD_{50} values close to GI_{50} values. MDA-MB-157 cells underwent cell death following Hsp90 inhibition with NVP-BEP800 but not NVP-AUY922, whereas SKBr3 and MCF-7 cells were resistant to cell killing by either agent (Table 2). The ability of either Hsp90 inhibitor to induce apoptosis was cell line dependent. Activated caspase-3/7 levels increased rapidly following exposure to five times the GI_{50} of NVP-BEP800 or NVP-AUY922 for 24 hours in BT-474 cells but not in any of the other breast cancer cell lines investigated (Fig. 1B). Apoptosis was confirmed by Western blot analysis for cleaved poly(ADP-ribose) polymerase. In previous studies, 17-AAG induced cell death in BT-474, MDA-MB-157, and BT20 cells, with caspase-dependent apoptosis observed only in the BT-474 cell line. All of the other four breast cancer cell lines tested (MDA-MB-231, MDA-MB-468, SKBr3, and MCF-7), while undergoing growth arrest, were resistant to cell killing by 17-AAG (26, 33). Significant apoptosis following NVP-BEP800 treatment was also observed in A2058 but not in HCT116 or A549 cells (data not shown).

Table 2. Antiproliferative and cytotoxic potential of NVP-BEP800 and NVP-AUY922 in a panel of human breast cancer cell lines

Cell line	ErbB2	ER	NVP-BEP800		NVP-AUY922	
			GI_{50} (nmol/L)	LD_{50} (nmol/L)	GI_{50} (nmol/L)	LD_{50} (nmol/L)
BT-474	+	+	53	45	3.1	3.7
SKBr3	+	–	56	>5,000	3.3	>400
MCF-7	–	+	118	>5,000	8.8	>400
MDA-MB-157	–	–	89	255	126	>400
MDA-MB-231	–	–	190	473	7.0	5.6
MDA-MB-468	–	–	173	59	6.3	3.2
BT20	–	–	162	360	4.0	4.3

Published OnlineFirst April 6, 2010; DOI: 10.1158/1535-7163.MCT-10-0055

NVP-BEP800 causes p23/Hsp90 dissociation and client protein degradation *in vitro*

The molecular signature of Hsp90 inhibitors includes the dissociation of Hsp90-p23 complexes, decrease of Hsp90 client proteins (such as Raf-1 and ErbB2), and transcriptional induction of Hsp70 expression. A method of studying Hsp90 inhibition, which closely monitors the catalytic cycle of Hsp90, is through evaluation of disruption of the Hsp90-p23 complex. Thus, destabilization of the Hsp90-p23 interaction in tumor cells and the subsequent measurement by immunoprecipitation can be used to monitor the effect of Hsp90 inhibitors directly on the target. At first, we evaluated the time course of Hsp90-p23 dissociation in A375 and BT-474 cells at a drug

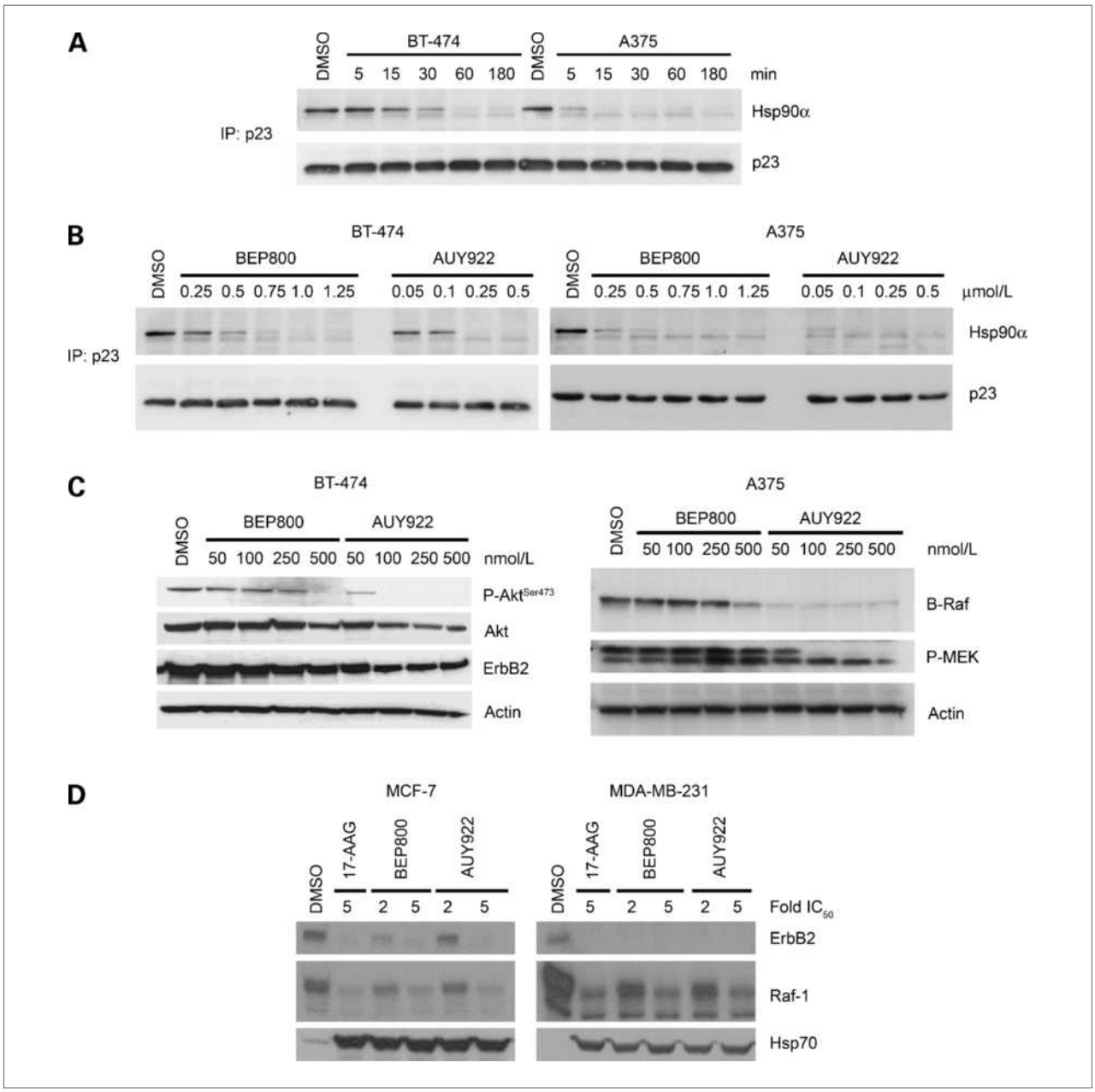

Figure 2. NVP-BEP800 depletes client proteins in human cancer cell lines *in vitro*. A, immunoblot of Hsp90 and p23 levels following immunoprecipitation of p23 in BT-474 or A375 cells treated with 500 nmol/L NVP-BEP800 for 5 min to 3 h. B, immunoblot of Hsp90 and p23 levels following immunoprecipitation of p23 in BT-474 cells treated with 250 to 1,250 nmol/L NVP-BEP800 or 50 to 500 nmol/L NVP-AUY922 for 3 h. C, Western blot analysis of BT-474 or A375 cells following 24-h exposure to 50 to 500 nmol/L NVP-BEP800 or NVP-AUY922. D, Western blot analysis of breast cancer cell lines MCF-7 or MDA-MB-231 following 24-h exposure to concentrations corresponding to two or five times the GI_{50} of NVP-BEP800 or NVP-AUY922, or five times the GI_{50} of 17-AAG.

Published OnlineFirst April 6, 2010; DOI: 10.1158/1535-7163.MCT-10-0055

concentration of 500 nmol/L (Fig. 2A). In BT-474 cells, complete dissociation was observed after between 30 and 60 minutes of incubation with NVP-BEP800. In A375 cells, only a minor fraction of Hsp90 was bound to p23 after 15 minutes of incubation. These data show that p23-Hsp90 dissociation occurs more rapidly in A375 compared with BT-474 cells. Next, the level of Hsp90-p23 dissociation in the presence of increasing concentrations of NVP-BEP800 or NVP-AUY922 was determined in comparison with a solvent (DMSO) control (Fig. 2B). An incubation time of 3 hours was chosen because maximum p23-Hsp90 dissociation was achieved in both A375 and BT-474 cells at this time point (Fig. 2A). In both cell lines, NVP-BEP800 and NVP-AUY922 caused a concentration-dependent decrease in the amount of Hsp90 coimmunoprecipitating with p23. In A375 cells, maximum dissociation of the Hsp90-p23 complex was achieved when incubated with 500 to 750 nmol/L NVP-BEP800 or 50 to 100 nmol/L NVP-AUY922. In the BT-474 cells, maximum Hsp90-p23 dissociation was achieved at 500 to 750 nmol/L NVP-BEP800 or 100 to 250 nmol/L NVP-AUY922. These data confirm the higher potency of NVP-AUY922 compared with NVP-BEP800. Following up on those results, the effect of NVP-BEP800 and NVP-AUY922 on levels of client proteins and their phosphorylation state was evaluated after 24 hours of incubation

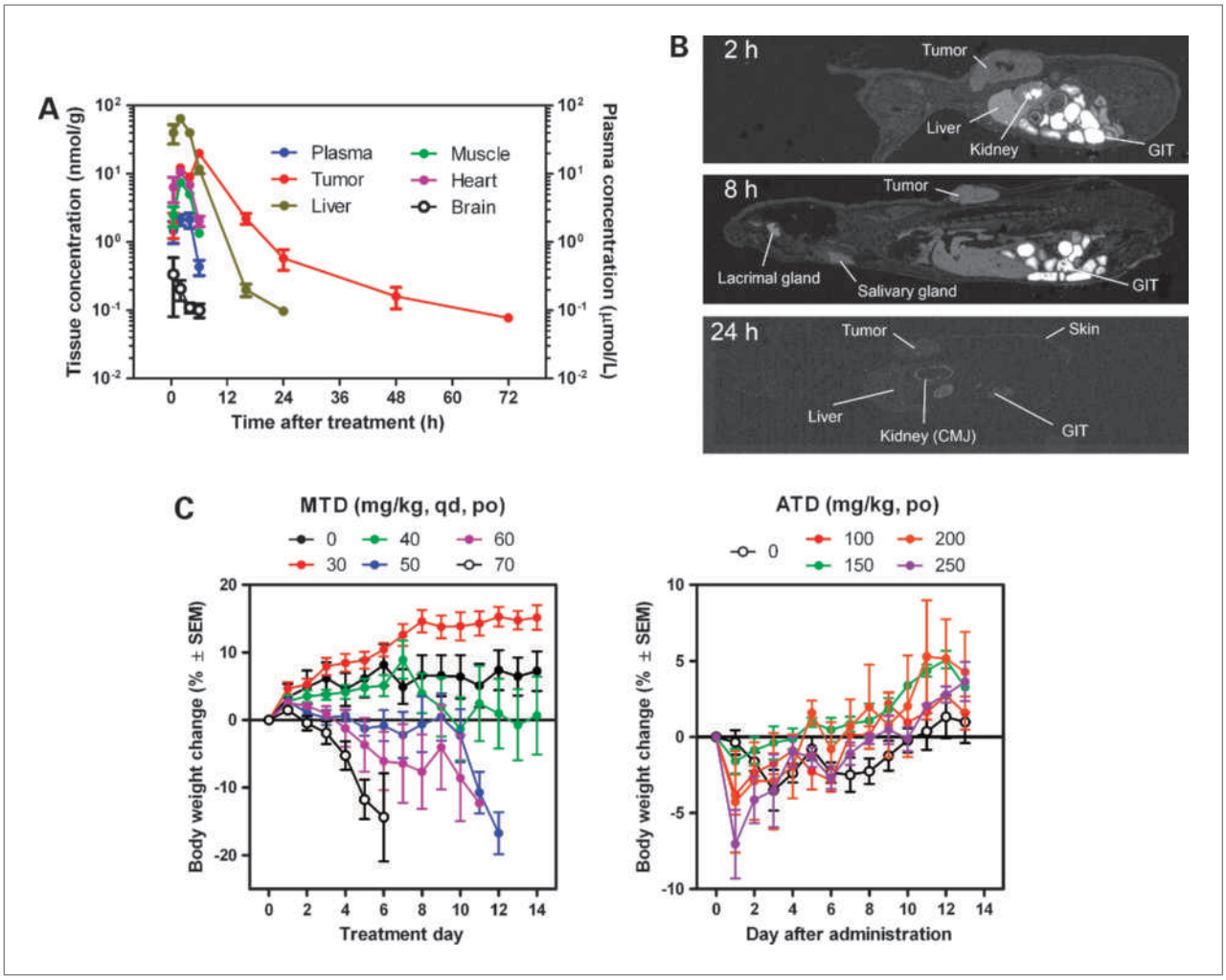

Figure 3. Bioavailability and tolerability of NVP-BEP800 in nude mice. A, pharmacokinetic profile of NVP-BEP800 in BT-474 tumor xenografts, plasma, and organs (liver, heart, brain, and skeletal muscle) after administration of a single dose. Female athymic mice bearing subcutaneous xenotransplants of the human ductal breast carcinoma BT-474 of ~250 mm^3 received a single oral dose of 30 mg/kg NVP-BEP800 at 0 h. NVP-BEP800 concentrations were determined by HPLC/MS-MS analysis using an internal standard method. Points, mean (n = 4); bars, SE. B, biodistribution determined by quantitative whole-body autoradioluminography. BT-474 tumor-bearing mice were orally administered 30 mg/kg ^{14}C-labeled NVP-BEP800 and distribution of radioactive material was measured by autoluminography. Sections taken 2, 8, and 24 h after administration are depicted. CMJ, cortico-medular junction. C, the MTD and ATD doses of NVP-BEP800 were determined. For determination of MTD, 0 to 70 mg/kg of NVP-BEP800 were administered daily via the oral route for 2 wk or until 15% body weight loss was observed. For ATD determination, a single dose (0–250 mg) was administered orally and body weights were monitored for 2 wk. Points, mean (n = 3); bars, SE.

Published OnlineFirst April 6, 2010; DOI: 10.1158/1535-7163.MCT-10-0055

Table 3. Pharmacokinetic parameters determined after administration of NVP-BEP800 at a dose of 30 mg/kg orally or 5 mg/kg i.v.

	Plasma	Tumor	Liver	Muscle	Heart	Brain
30 mg/kg, orally						
C_{max} ± SEM (μmol/L), tissue (nmol/g)	2.1 ± 0.5	19.9 ± 1.9	64.1 ± 7.8	7.4 ± 0.8	10.6 ± 0.6	0.3 ± 0.3
T_{max} (h)	4	6	2	4	4	0.5
$T_{1/2}$ elimination λ_z (h)	1.7	16.4	2.1	1.6	1.6	3
AUC (0–∞) (h · μmol/L), tissue (h · nmol/g)	10.5	163	265	29.1	44.2	1.4
AUC tissue/plasma ratio	—	15.5	25.2	2.8	4.2	0.1
5 mg/kg, i.v.						
C_{max} ± SEM (μmol/L), tissue (nmol/g)	—	6.6 ± 0.1	33 ± 2.3	6.4 ± 0.7	22 ± 3.4	0.18 ± 0.04
T_{max} (h)	—	1	0.25	0.25	0.083	0.25
$T_{1/2}$ elimination λ_z (h)	1.4	5	2.6	1.1	3	1.7
AUC (0–∞) (h · μmol/L), tissue (h · nmol/g)	2.2	40	50	10.3	16.5	0.44
%F	80					

NOTE: The highest concentration (C_{max}), terminal half-life ($T_{1/2}$ elimination λ_z, after oral dose, apparent), and exposure as determined by AUC were determined for each organ, plasma, and BT-474 xenograft (tumor). Bioavailability (%F) was determined based on dose-normalized plasma exposures.

(Fig. 2C). NVP-BEP800 and NVP-AUY922 induced a concentration-dependent decrease in phospho-Akt (Ser^{473}) and ErbB2 levels in BT-474 cells. Phosphorylation of Akt at Ser^{473} was not detectable at 500 nmol/L NVP-BEP800 or 100 nmol/L NVP-AUY922, and lower levels of Akt and ErbB2 were detected at those concentrations. Similarly, in A375 cells, B-Raf(V600E) decreased in A375 melanoma cells at 500 nmol/L NVP-BEP800 and <50 nmol/L NVP-AUY922 (Fig. 2C). In addition, slightly decreased MEK phosphorylation was observed at 500 nmol/L NVP-BEP800 and no detectable phosphorylation was detected at 100 nmol/L NVP-AUY922. Comparing equi-cell growth-inhibitory concentrations of NVP-BEP800 and NVP-AUY922, no discernable difference in client protein

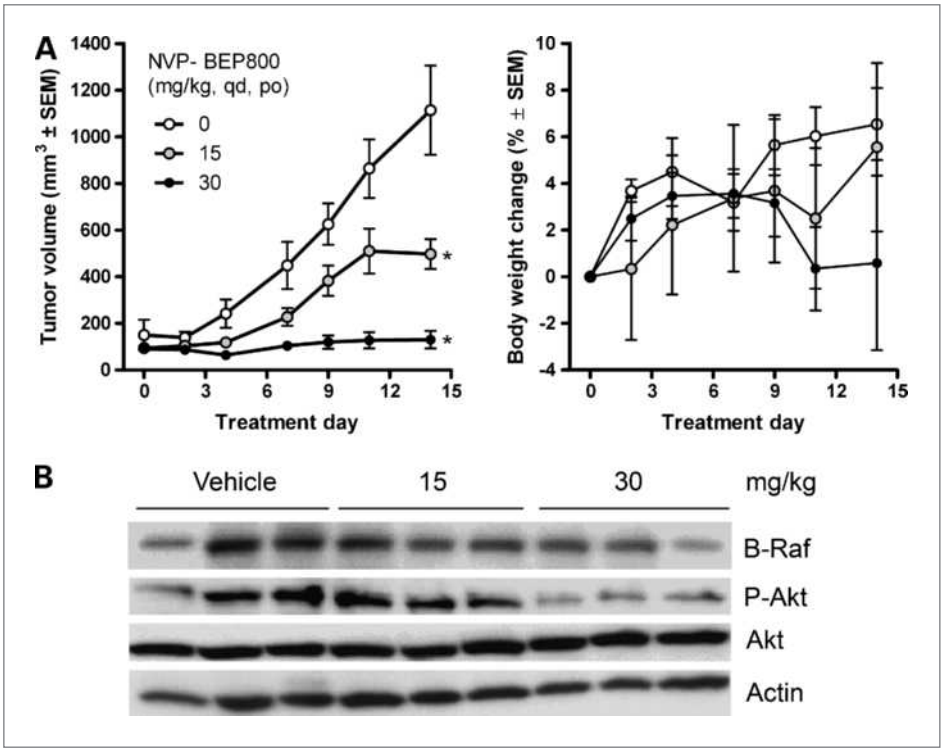

Figure 4. Antitumor efficacy, tolerability, and pharmacodynamic effects of NVP-BEP800 in the A375 melanoma xenograft model. A375 cells were inoculated s.c. in female nude mice. When the tumors reached 100 to 200 mm^3, drug treatment was initiated. Each group consisted of eight animals (n = 8). A, NVP-BEP800 was administered daily at dose levels of 15 or 30 mg/kg orally. Tumor volumes and body weights were measured thrice per week. Points, mean; bars, SE. *, $P < 0.05$, one-way ANOVA post hoc Dunnett, statistical significance compared with vehicle-treated controls. B, tumors were dissected 8 h after the last treatment and pharmacodynamic response of B-Raf, phospho-Akt (P-Akt), and Akt was analyzed by Western blot analysis. Actin was used as a loading control.

Published OnlineFirst April 6, 2010; DOI: 10.1158/1535-7163.MCT-10-0055

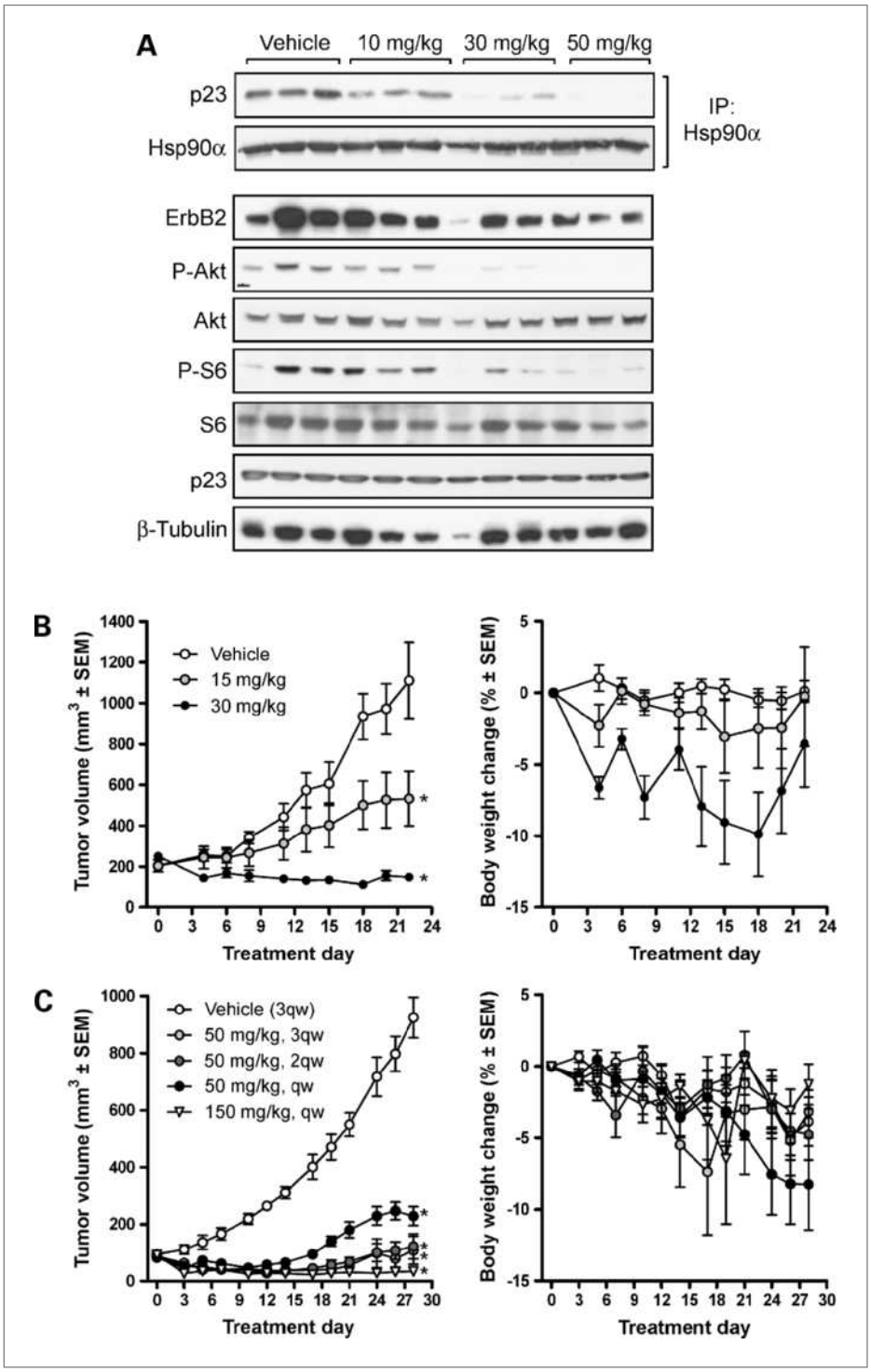

Figure 5. Antitumor efficacy, tolerability, and pharmacodynamic effects of NVP-BEP800 in the BT-474 human breast cancer xenograft model. BT-474 cells were inoculated s.c. in female nude mice carrying an estrogen-release pellet. When the tumors reached 100 to 250 mm^3, drug treatment was initiated. Each group consisted of eight animals. A, NVP-BEP800 was administered daily at dose levels of 10, 30, or 50 mg/kg orally for 1 wk. Tumors were dissected 8 h after the last treatment, and pharmacodynamic responses on Hsp90/p23 association, ErbB2, phospho-Akt, Akt, P-S6, and S6 were analyzed by coimmunoprecipitation and Western blot analysis. β-Tubulin was used as a loading control. B, 15 or 30 mg/kg of NVP-BEP800 were administered daily orally. Tumor volumes and body weights were measured thrice per week. Points, mean; bars, SE. C, NVP-BEP800 (50 mg/kg) was administered orally thrice per week (3qw; Monday, Wednesday, and Friday), twice per week (2qw; Tuesday and Friday), or once per week (qw; Friday). One group was administered 150 mg/kg once per week (Friday). Dosing was initiated on a Friday (day 0). Asterisks indicate statistical significance compared with vehicle-treated controls ($P < 0.05$, one-way ANOVA post hoc Dunnett).

degradation was observed (Fig. 2D). In the breast cancer cell lines MCF-7 and MDA-MB-231, five times the GI_{50} of NVP-BEP800 and NVP-AUY922 induced degradation of ErbB2 and Raf-1 and upregulation of Hsp70 (Fig. 2D). Using In-Cell-Western technology, the IC_{50} was determined to be 218 nmol/L for Akt dephosphorylation, 39.5 nmol/L for ErbB2 dephosphorylation, 137 nmol/L for ErbB2 degradation, and 207 nmol/L for Hsp70 induction following a 6-hour exposure of BT-474 cells to NVP-BEP800. NVP-BEP800 showed *in vitro* pharmacodynamic marker responses, consistent with Hsp90 inhibition but with lower potency than NVP-AUY922.

Published OnlineFirst April 6, 2010; DOI: 10.1158/1535-7163.MCT-10-0055

Pharmacokinetic profile of NVP-BEP800 in tumor-bearing mice

NVP-BEP800 was optimized for oral bioavailability (21). The pharmacokinetic profile of NVP-BEP800 was determined following oral and i.v. administration to BT-474 xenograft-bearing athymic mice. The mean plasma, tumor, and tissue concentrations versus time curves for NVP-BEP800 following a single oral dose of 30 mg/kg are depicted in Fig. 3A, whereas the pharmacokinetic parameters derived from these data, and a single i.v. dose of 5 mg/kg, are summarized in Table 3. NVP-BEP800, following a single 30 mg/kg oral dose, was readily absorbed, achieving a T_{max} of ~4 hours and a peak plasma concentration of 2.1 μmol/L. The oral bioavailability (%F) of NVP-BEP800 was 80%. NVP-BEP800 rapidly distributed from blood into peripheral tissues. Volume of distribution was 7.0 L/kg, and the plasma clearance was relatively high (4.7 L/h/kg; calculated from i.v. dose; data not shown). High systemic exposure was further confirmed by comparing the ratio of AUC in tissues to plasma. For the muscle and heart, 3- to 4-fold higher exposure was determined. The liver-to-plasma AUC ratio was 25 and was accompanied by a short apparent terminal elimination half-life of between 1.6 and 2.1 hours. Tumor tissue also showed a high tissue-to-plasma AUC ratio of 16, but compared with tissues, the apparent terminal elimination half-life was significantly increased to 16.4 hours.

Whole-body autoradiography, following a single oral dose of 30 mg/kg [^{14}C]NVP-BEP800 to BT-474 tumor-bearing athymic mice, further confirmed these observations (Fig. 3B). T_{max} was achieved in most tissues, including the tumor, at 4 hours after dose. Up to 4 hours after dose, the highest levels of total radiolabeled components were found in the bile, indicating biliary excretion. At T_{max}, high radioactivity concentrations were observed in the Harderian gland, lacrimal gland, duodenal wall, glandular stomach mucosa, liver, salivary gland, pelvis, and lung (data not shown). From 8 hours after dose, radioactive material was eliminated rapidly from most tissues. At 24 hours after dose, concentrations >LOD were detected only in the kidney cortico-medullar junction and cortex, lacrimal gland, Harderian gland, tumor, liver, skin, and brown fat. No radioactivity was detected in the body at 168 hours after dose. The uptake of total radiolabeled components into the tumor occurred slowly. In the time interval 2 to 8 hours after dose, the radioactivity concentrations in the tumor were 6- to 15-fold higher than in blood. As previously observed, no significant brain uptake could be detected (an AUC brain-to-blood ratio lower than 0.1 indicates poor blood-brain barrier penetrance of NVP-BEP800).

Tolerability of NVP-BEP800 in nude mice

Based on the pharmacokinetic profile of NVP-BEP800, a daily dosing schedule was initially selected. The maximum tolerated dose (MTD) was determined following administration of 30 to 70 mg/kg daily for 14 days to female nude mice in groups of three animals (Fig. 3C). Dose levels above 40 mg/kg caused excessive body weight loss, whereas 40 mg/kg was well tolerated and was set as the MTD in a daily dosing regimen. The group treated at 30 mg/kg had higher body weight gain than the vehicle-treated control group in this experiment. However, this was not generally observed (see Figs. 4A, 5B, and 5C). The acute tolerated dose (ATD) was determined by administering a single dose up to 250 mg/kg. All doses were relatively well tolerated with a maximum mean body weight loss of 7%. Thus, the ATD is higher than 250 mg/kg in nude mice.

Antitumor effect of NVP-BEP800 in xenograft models

NVP-BEP800 was tested for antitumor efficacy against human tumor xenografts in nude mice. Malignant melanoma remains one of the deadliest tumor types, and effective therapies are lacking. Recent reports have identified activating mutations in the human *B-Raf* gene in up to 80% of melanomas (34). Given the prevalence of B-Raf mutations in melanoma, there is a good rationale to develop therapies targeting the Ras/Raf/MEK/mitogen-activated protein kinase signaling cascade. It is well established that Raf kinase family members are Hsp90 client proteins, and therefore, Hsp90 inhibition in melanoma cells should diminish Ras signaling and simultaneously affect other pathways critical for growth and survival of the tumor cell. The human melanoma cell line A375 expresses activated B-Raf^{V600E}. A375

Table 4. Summary of A375 tumor responses and tolerability evaluated 15 d after the first dose

Compound	Dose, route, schedule	Tumor response		Host response		Survival
		T/C (%)	ΔTumor volume	ΔBody weight	ΔBody weight (%)	
Vehicle	10 mL/kg, once daily, orally	100	2,398 ± 425	1.7 ± 0.4	6.5 ± 1.5	8/8
BEP800	15 mg/kg, once daily, orally	53	1,276 ± 186	1.3 ± 1.0	5.5 ± 3.6	8/8
BEP800	30 mg/kg, once daily, orally	6	156 ± 114	0.1 ± 1.0	0.6 ± 3.7	8/8

NOTE: The percentage T/C is calculated as the mean change in tumor volume of the treated group divided by the mean change in tumor volume of the vehicle-treated control group.

Published OnlineFirst April 6, 2010; DOI: 10.1158/1535-7163.MCT-10-0055

xenograft-bearing mice were treated daily with NVP-BEP800 at 15 or 30 mg/kg/d (Fig. 4). Significant antitumor efficacy ($P < 0.05$) was observed at both dose levels, with 30 mg/kg/d causing near stasis (Fig. 4A). On the final treatment day, the observed T/C values were 53% and 6% for the 15 and 30 mg/kg groups, respectively (Table 4). The treatment regimens were well tolerated and the mean body weights increased during the study in all groups. However, less body weight gain was observed at the 30 mg/kg/d (0.1 ± 1 g) compared with vehicle-treated animals (6.5 ± 3.7 g; Table 4). At the end of the antitumor efficacy study (8 hours after the last treatment), xenografts were dissected and processed for Western blot analysis (Fig. 4B). No change in the levels of total Akt could be detected (Fig. 4B). However, a dose-dependent reduction in B-Raf and Akt phosphorylation levels was observed with strong reduction at the 30 mg/kg dose level. These data are consistent with the dose-dependent antitumor efficacy observed in the A375 melanoma model.

Antitumor activity was also observed in BT-474 breast cancer xenografts. This model is frequently used to study the antitumor effect of Hsp90 inhibitors due to high expression of the well-described client proteins ErbB2 and ER (26). Initially, we determined the effect of NVP-BEP800 on pharmacodynamic markers when administered to athymic female nude mice bearing BT-474 tumor xenografts orally for 1 week daily at 10, 30, or 50 mg/kg (Fig. 5A). The tumors were dissected 8 hours after the final treatment and processed for Western blot analysis. A dose-dependent effect was observed on Hsp90-p23 complex dissociation, with no detectable p23 protein bound to Hsp90 at the 50 mg/kg dose level. Consistent with this, dose-dependent reductions in the steady-state ErbB2 levels and levels of phospho-Akt and phospho-S6 were observed. No appreciable reduction in Akt was detected. Next, the antitumor efficacy was determined in BT-474 xenograft-bearing mice treated daily for 22 days at dose levels of 15 or 30 mg/kg/d (Fig. 5B). Statistically significant ($P < 0.05$) antitumor effect was observed when treated at dose levels of 15 or 30 mg/kg/d (Fig. 5B). The highest dose level caused 38% regression, whereas 15 mg/kg/d resulted in a T/C of 36%.

To further explore the dosing schedule for NVP-BEP800, several treatment regimens were evaluated. Treatment with 50 mg/kg, once daily for 1 week, was tolerated (Fig. 3B) and resulted in a strong effect of pharmacodynamic markers (Fig. 5A). This dose was evaluated when administered one, two, or three times per week. In addition, one group was treated with 150 mg/kg NVP-BEP800 once per week (Fig. 5C). This group received the same total weekly dose as the group treated three times per week but would achieve a higher C_{max}. All treatment regimens resulted in statistically significant efficacy ($P < 0.05$); however, increasing dosing frequency seemed to result in increased efficacy. One weekly dose of 50 mg/kg gave a T/C value of 19%, whereas two and three 50 mg/kg doses resulted in T/Cs of 4% and 3%, respectively. Once weekly administration of 150 mg/kg resulted in statistically significant smaller tumors than 50 mg/kg, whereas no statistically significant difference was detected between other treatment groups. The most efficacious dosing regimen was a single weekly bolus of 150 mg/kg, which resulted in regression of 62%. These data indicate that reaching a high C_{max} is important for efficacy, although this also could lead to increased toxicity. Administering a total weekly dose of 150 mg/kg either in one bolus or split in three doses of 50 mg/kg resulted in toxicity. Four of eight animals survived to the end of the experiment when three doses per week of 50 mg/kg were given compared with six animals with a single weekly dose of 150 mg/kg. The average body weight loss was not statistically significantly different from that observed in the control group. However, because the animals with the greatest body weight losses were sacrificed during the study, the actual body weight loss would have been higher had they remained in the study. All animals survived without significant body weight loss when treated with 50 mg/kg once or twice per week.

Discussion

The paradigm of "oncogenic addiction," where individual cancers are believed to be driven by definable oncogenic events, has resulted in the age of "molecular targeted therapeutics." There have been some unparalleled successes in the development of molecularly targeted agents (i.e., imatinib for Philadelphia chromosome–positive chronic myelogenous leukemia and acute lymphoblastic leukemia and trastuzumab for Her2-positive breast cancer). However, a large number of targeted kinase inhibitors, such as those targeting receptor tyrosine kinases (e.g., sunitinib, sorafenib, gefitinib, or erlotinib) or their downstream signaling cascades (e.g., MEK or mammalian target of rapamycin inhibitors), while receiving approval in some cases for use in less common malignancies, have not quite lived up to their promise. The complex network-dependent nature of these signaling pathways with multiple interpathway cross talk and feedback loops suggests that many tumors are not dependent on a single pathway and targeting multiple signaling nodes could be critical to gaining therapeutic benefit from targeted agents. Through its ability to control the activity and stability of multiple oncogenic signaling proteins, inhibitors of Hsp90 have the potential to inhibit multiple signaling pathways. The targeting of Hsp90 has therefore been seized on as an important strategy for developing novel cancer therapeutics.

NVP-BEP800 is a novel, fully synthetic, orally bioavailable small-molecule inhibitor of Hsp90 discovered through a combination of fragment-based and *in silico* screening and structure-guided drug design (21). In binding assays, NVP-BEP800 bound competitively with a resorcinol-based fluorescent probe to the ATPase site of Hsp90, with an IC_{50} of 58 nmol/L. This was less potent than NVP-AUY922 (33) but comparable with other oral

Published OnlineFirst April 6, 2010; DOI: 10.1158/1535-7163.MCT-10-0055

Hsp90 inhibitors such as BIIB021 and CUDC-305 (35, 36). NVP-BEP800 showed selectivity versus the related GHKL ATPases Grp94 and Trap-1 of >70-fold. This is the first small-molecule Hsp90 inhibitor to show such selectivity. In comparison, NVP-AUY922 showed 25-fold selectivity versus Grp94 and 3.8-fold versus Trap-1. The selectivity of other agents versus these two Hsp90 orthologues has yet to be described. Grp94 is expressed predominantly in the endoplasmic reticulum and Trap-1 in the mitochondria. These chaperones, especially Trap-1, have been less studied than Hsp90, and the possibility exists that inhibiting them could increase the systemic toxicity of Hsp90 inhibitors. Close analogues of NVP-BEP800 have been identified that exhibit reduced selectivity to Grp94 and Trap-1 (e.g., 34a in ref. 21 shows ~8-fold selectivity for Hsp90 versus Grp94 and Trap-1). This compound shows similar efficacy and tolerability to NVP-BEP800 in xenograft-bearing nude mice. Further clinical evaluation is needed to determine whether this selectivity translates into an improved therapeutic index.

NVP-BEP800 inhibited tumor cell proliferation *in vitro* with an average GI_{50} of 245 nmol/L compared with 10.7 nmol/L for NVP-AUY922, one of the most potent Hsp90 inhibitors described to date (22, 26, 33). In addition to inhibiting the proliferation of human tumor cells *in vitro*, NVP-BEP800 inhibited the proliferation of hematopoietic stem cells growing in culture with approximate equipotency. This has been described previously with other Hsp90 inhibitors, including 17-AAG and NVP-AUY922, and likely reflects the dependence of these cell lines on growth factor signaling pathways for their proliferation. The "oncogene addiction" paradigm suggests that cancer cells rely on these pathways for their survival, whereas normal cells rely on these pathways for proliferation but not survival. Therefore, the identification of a nontoxic, therapeutically active dose of NVP-BEP800 should be achievable. The hallmarks of Hsp90 inhibition include upregulation of Hsp70 and destabilization followed by proteasomal degradation of client proteins involved in oncogenic signaling. NVP-BEP800 induced the degradation of key client proteins, including ErbB2, Akt, Raf-1, and B-Raf(V600E), in A375 melanoma cells and BT-474, MCF-7, and MDA-MB-231 breast carcinoma cells at concentrations that induced growth arrest. Inhibition of key downstream signaling pathways was also detectable through the dose-dependent inhibition of Akt, MEK, and S6 phosphorylation.

When administered via the oral route, NVP-BEP800 exhibited good bioavailability of ~80% in tumor-bearing nude mice. Pharmacokinetic analysis indicated that NVP-BEP800 had a relatively short apparent terminal half-life of 1.7 hours in plasma but selective retention in tumors with an extended half-life of 16.4 hours. High liver exposure of NVP-BEP800 was observed in tissue distribution studies. However, clearance of NVP-BEP800 from all tissues was much more rapid than tumor with half-life of 1.6 to 3 hours, and no hepatotoxicity was observed in the preclinical toxicology studies (data not shown). The phenomenon of high liver exposure has also been observed with CUDC-305 (35), but in comparison with NVP-BEP800, CUDC-305 had a long liver retention time resulting in a reduced tumor to liver half-life ratio. NVP-BEP800 exhibited no appreciable brain penetrance, suggesting that central nervous system toxicities should not be an issue for this molecule. The long tumor retention time versus rapid plasma and normal tissue clearance suggests that frequent dosing of NVP-BEP800 enabling the continual inhibition of Hsp90 in the tumor without systemic toxicity should be achievable.

When administered orally in a daily schedule, the MTD was determined as 40 mg/kg, whereas a single dose of NVP-BEP800 was well tolerated at >250 mg/kg. This indicates that an NVP-BEP800 overdose may be relatively well tolerated, although the absorption and pharmacokinetic profile have not been studied at such high doses. NVP-BEP800 induced tumor stasis or regression in BT-474 xenograft-bearing nude mice when administered using a once, twice, or thrice weekly or daily schedule. As predicted from the pharmacokinetic data, the optimal tumor growth inhibition versus tolerability was observed following daily oral dosing in both the BT-474 breast and A375 melanoma xenograft models. This tumor growth inhibition corresponded with robust client protein modulation in both tumor models. CUDC-305 and BIIB021 exhibit similar affinity for Hsp90 and inhibit tumor cell growth to an equivalent extent as NVP-BEP800. They are highly orally bioavailable (35, 36) yet require significantly higher doses of compound to inhibit tumor growth to the same extent as NVP-BEP800. For example, 30 mg/kg daily dosing of NVP-BEP800 induces tumor regression in BT-474 xenograft models, whereas 120 mg/kg daily BIIB021 and 160 mg/kg twice daily CUDC-305 are required to induce similar tumor responses. This is likely a reflection of the superior pharmacokinetic properties of NVP-BEP800, allowing high tumor levels with low systemic toxicity to be achieved.

There are currently 3 ansamycin (tanespimycin, retaspimycin, and IPI-493) and at least 11 non-ansamycin (6 oral and 5 i.v.) agents in clinical trials (5, 37). Tanespimycin (17-AAG) was the first inhibitor of Hsp90 to enter clinical trials but suffers from serious limitations, including hepatotoxicity, poor water solubility requiring complex formulations, tumor expression of NQO1 for activity, limited bioavailability, and efflux by P-glycoprotein. The issues associated with formulation have largely been resolved with the introduction of the hydroquinone prodrug retaspimycin (IPI-504). Because NVP-BEP800 is a novel, non-ansamycin inhibitor of Hsp90, it does not have the limitations associated with tanespimycin and its analogues. Despite showing target modulation, neither tanespimycin nor retaspimycin has achieved significant clinical activity to date (5). Recent advances suggest that Hsp90 inhibitors could have the most therapeutic potential when used in combination. Clinical trials of tanespimycin in combination with bortezomib in multiple myeloma and tyrosine kinase

Published OnlineFirst April 6, 2010; DOI: 10.1158/1535-7163.MCT-10-0055

inhibitors in non–small cell lung carcinoma are exploring this. Agents such as NVP-BEP800 that show *in vivo* activity when administered on a range of schedules from once weekly to once daily should make the identification of optimal combination dosing schedules and the management of overlapping toxicities much more manageable.

When administered at the right dose and optimal schedule, all Hsp90 inhibitors described to date show robust inhibition of tumor growth in xenograft models. However, all have different pharmacokinetic properties and are likely to show overlapping yet differential toxicologic profiles. Only once these agents have been explored more fully in a clinical setting as single agents and in combination with other treatment modalities will it become clear which have the optimal profiles. NVP-BEP800, with its potent antitumor activity, optimal pharmacokinetic profile, favorable safety profile, and differential dosing schedules, warrants further clinical evaluation.

Disclosure of Potential Conflicts of Interest

No potential conflicts of interest were disclosed.

Acknowledgments

We thank Jacqueline Bohn, Kerstin Pollehn, Joëlle Rubert, Dario Sterker, Sonja Tobler, Arlette Wach, and Axelle Welsch for their excellent technical assistance and dedication to the project.

The costs of publication of this article were defrayed in part by the payment of page charges. This article must therefore be hereby marked *advertisement* in accordance with 18 U.S.C. Section 1734 solely to indicate this fact.

Received 09/28/2010; revised 01/18/2010; accepted 02/16/2010; published OnlineFirst 04/06/2010.

References

1. Taldone T, Sun W, Chiosis G. Discovery and development of heat shock protein 90 inhibitors. Bioorg Med Chem 2009;17:2225–35.
2. Koga F, Kihara K, Neckers L. Inhibition of cancer invasion and metastasis by targeting the molecular chaperone heat-shock protein 90. Anticancer Res 2009;29:797–807.
3. Workman P, Burrows F, Neckers L, Rosen N. Drugging the cancer chaperone HSP90: combinatorial therapeutic exploitation of oncogene addiction and tumor stress. Ann N Y Acad Sci 2007;1113:202–16.
4. Drysdale MJ, Brough PA, Massey A, Jensen MR, Schoepfer J. Targeting Hsp90 for the treatment of cancer. Curr Opin Drug Discov Devel 2006;9:483–95.
5. Gao Z, Garcia-Echeverria C, Jensen MR. Hsp90 inhibitors: clinical development and future opportunities in oncology therapy. Curr Opin Drug Discov Devel 2010;13:193–202.
6. Dutta R, Inouye M. GHKL, an emergent ATPase/kinase superfamily. Trends Biochem Sci 2000;25:24–8.
7. Dollins DE, Warren JJ, Immormino RM, Gewirth DT. Structures of GRP94-nucleotide complexes reveal mechanistic differences between the hsp90 chaperones. Mol Cell 2007;28:41–56.
8. Saibil HR. Chaperone machines in action. Curr Opin Struct Biol 2008;18:35–42.
9. Hanahan D, Weinberg RA. The hallmarks of cancer. Cell 2000;100:57–70.
10. Maloney A, Workman P. HSP90 as a new therapeutic target for cancer therapy: the story unfolds. Expert Opin Biol Ther 2002;2:3–24.
11. Pratt WB, Toft DO. Regulation of signaling protein function and trafficking by the hsp90/hsp70-based chaperone machinery. Exp Biol Med (Maywood) 2003;228:111–33.
12. Taldone T, Gozman A, Maharaj R, Chiosis G. Targeting Hsp90: small-molecule inhibitors and their clinical development. Curr Opin Pharmacol 2008;8:370–4.
13. Egorin MJ, Zuhowski EG, Rosen DM, Sentz DL, Covey JM, Eiseman JL. Plasma pharmacokinetics and tissue distribution of 17-(allylamino)-17-demethoxygeldanamycin (NSC 330507) in CD2F1 mice1. Cancer Chemother Pharmacol 2001;47:291–302.
14. Glaze ER, Lambert AL, Smith AC, et al. Preclinical toxicity of a geldanamycin analog, 17-(dimethylaminoethylamino)-17-demethoxygeldanamycin (17-DMAG), in rats and dogs: potential clinical relevance. Cancer Chemother Pharmacol 2005;56:637–47.
15. Supko JG, Hickman RL, Grever MR, Malspeis L. Preclinical pharmacologic evaluation of geldanamycin as an antitumor agent. Cancer Chemother Pharmacol 1995;36:305–15.
16. Solit DB, Ivy SP, Kopil C, et al. Phase I trial of 17-allylamino-17-demethoxygeldanamycin in patients with advanced cancer. Clin Cancer Res 2007;13:1775–82.
17. Guo W, Reigan P, Siegel D, Zirrolli J, Gustafson D, Ross D. Formation of 17-allylamino-demethoxygeldanamycin (17-AAG) hydroquinone by NAD(P)H:quinone oxidoreductase 1: role of 17-AAG hydroquinone in heat shock protein 90 inhibition. Cancer Res 2005;65:10006–15.
18. Guo W, Reigan P, Siegel D, Zirrolli J, Gustafson D, Ross D. The bioreduction of a series of benzoquinone ansamycins by NAD(P)H: quinone oxidoreductase 1 to more potent heat shock protein 90 inhibitors, the hydroquinone ansamycins. Mol Pharmacol 2006;70:1194–203.
19. Kelland LR, Sharp SY, Rogers PM, Myers TG, Workman P. DT-Diaphorase expression and tumor cell sensitivity to 17-allylamino, 17-demethoxygeldanamycin, an inhibitor of heat shock protein 90. J Natl Cancer Inst 1999;91:1940–9.
20. Gaspar N, Sharp SY, Pacey S, et al. Acquired resistance to 17-allylamino-17-demethoxygeldanamycin (17-AAG, tanespimycin) in glioblastoma cells. Cancer Res 2009;69:1966–75.
21. Brough PA, Barril X, Borgognoni J, et al. Combining hit identification strategies: fragment-based and *in silico* approaches to orally active 2-aminothieno[2,3-*d*]pyrimidine inhibitors of the Hsp90 molecular chaperone. J Med Chem 2009;52:4794–809.
22. Brough PA, Aherne W, Barril X, et al. 4,5-Diarylisoxazole Hsp90 chaperone inhibitors: potential therapeutic agents for the treatment of cancer. J Med Chem 2008;51:196–218.
23. Schilb A, Riou V, Schoepfer J, et al. Development and implementation of a highly miniaturized confocal 2D-FIDA-based high-throughput screening assay to search for active site modulators of the human heat shock protein 90β. J Biomol Screen 2004;9:569–77.
24. Chene P, Rudloff J, Schoepfer J, et al. Catalytic inhibition of topoisomerase II by a novel rationally designed ATP-competitive purine analogue. BMC Chem Biol 2009;9:1.
25. Smith V, Sausville EA, Camalier RF, Fiebig HH, Burger AM. Comparison of 17-dimethylaminoethylamino-17-demethoxy-geldanamycin (17DMAG) and 17-allylamino-17-demethoxygeldanamycin (17AAG) *in vitro*: effects on Hsp90 and client proteins in melanoma models. Cancer Chemother Pharmacol 2005;56:126–37.
26. Jensen MR, Schoepfer J, Radimerski T, et al. NVP-AUY922: a small molecule HSP90 inhibitor with potent antitumor activity in preclinical breast cancer models. Breast Cancer Res 2008;10:R33.
27. Hamaoka T. Autoradiography of new era replacing traditional X-ray film. Cell Technology 1990;9:456–62.
28. Ullberg S. The technique of whole-body autoradiography: cryosectioning of large specimens. Sweden: LKB-Producter AB; 1977.

Published OnlineFirst April 6, 2010; DOI: 10.1158/1535-7163.MCT-10-0055

29. Schweitzer A, Fahr A, Niederberger W. A simple method for the quantitation of ^{14}C-whole-body autoradiograms. Int J Rad Appl Instrum A 1987;38:329–33.
30. Giard DJ, Aaronson SA, Todaro GJ, et al. *In vitro* cultivation of human tumors: establishment of cell lines derived from a series of solid tumors. J Natl Cancer Inst 1973;51:1417–23.
31. Gershwin ME, Ikeda RM, Kawakami TG, Owens RB. Immunobiology of heterotransplanted human tumors in nude mice. J Natl Cancer Inst 1977;58:1455–61.
32. Tomayko MM, Reynolds CP. Determination of subcutaneous tumor size in athymic (nude) mice. Cancer Chemother Pharmacol 1989;24:148–54.
33. Eccles SA, Massey A, Raynaud FI, et al. NVP-AUY922: a novel heat shock protein 90 inhibitor active against xenograft tumor growth, angiogenesis, and metastasis. Cancer Res 2008;68:2850–60.
34. Thomas NE. BRAF somatic mutations in malignant melanoma and melanocytic naevi. Melanoma Res 2006;16:97–103.
35. Bao R, Lai CJ, Qu H, et al. CUDC-305, a novel synthetic HSP90 inhibitor with unique pharmacologic properties for cancer therapy. Clin Cancer Res 2009;15:4046–57.
36. Lundgren K, Zhang H, Brekken J, et al. BIIB021, an orally available, fully synthetic small-molecule inhibitor of the heat shock protein Hsp90. Mol Cancer Ther 2009;8:921–9.
37. Kim YS, Alarcon SV, Lee S, et al. Update on Hsp90 inhibitors in clinical trial. Curr Top Med Chem 2009;9:1479–92.

Published OnlineFirst April 6, 2010; DOI: 10.1158/1535-7163.MCT-10-0055

Molecular Cancer Therapeutics

Preclinical Antitumor Activity of the Orally Available Heat Shock Protein 90 Inhibitor NVP-BEP800

Andrew J. Massey, Joseph Schoepfer, Paul A. Brough, et al.

Mol Cancer Ther Published OnlineFirst April 6, 2010.